



Lucy Kettlewell. *Mount Equinox*. Oil on board. From the personal collection of John Horton.

*New techniques in radiotherapy for thoracic cancer patients show promise in sparing normal functional lung volumes while delivering adequate radiation dose to the tumors.*

## Functional Lung Imaging in Thoracic Cancer Radiotherapy

Geoffrey Zhang, PhD, Thomas J. Dilling, MD, Craig W. Stevens, MD, PhD, and Kenneth M. Forster, PhD

**Background:** Lung cancer is the No. 1 cancer killer of both men and women in the United States. Radiotherapy is frequently employed as part of the treatment. However, radiation must traverse surrounding regions of normal lung, potentially inducing pulmonary toxicity. Because these patients frequently have underlying lung disease, a radiation-induced decrement in lung function could be highly morbid or even fatal. It is well known that lung function is not uniform, with wide ranges of ventilation and perfusion levels throughout the lung. Currently radiation oncologists do not have the ability to account for this variation when generating treatment plans.

**Methods:** This article reviews some techniques used to assess pulmonary ventilation and perfusion, including nuclear medicine, magnetic resonance imaging (MRI) and computed tomography (CT).

**Results:** Many techniques have the potential to be used in radiotherapy treatment planning for thoracic cancer patients to spare normal functional lung volumes while delivering adequate radiation dose to the tumors. The article outlines a promising new technique to generate 3-D ventilation maps by using deformable image registration of 4-D CT image sets.

**Conclusions:** While there are some technical challenges to overcome before pulmonary functional imaging can be routinely employed clinically in radiation oncology, there is the potential to preferentially spare better perfused/ventilated regions of normal lung, which promises to reduce pulmonary toxicity.

### Introduction

According to the American Cancer Society, cancer is the second-leading cause of death in the United States after heart disease, accounting for 1 out of every 4 deaths.<sup>1</sup> Twenty-nine percent of these deaths are caused by lung cancer, making it the biggest single cancer killer of both men and women.<sup>1</sup> These tumors are generally in an advanced stage at diagnosis, thus diminishing the possibility for cure. Treatment options typically include surgery, chemotherapy, and radiotherapy, whether singly or in combination. Radiotherapy is utilized in up to half of lung cancer patients at some point after their cancer diagnosis.

---

From the Radiation Oncology Program at the H. Lee Moffitt Cancer Center & Research Institute, Tampa, Florida.

Submitted December 3, 2007; accepted January 30, 2008.

Address correspondence to Geoffrey Zhang, PhD, Radiation Oncology Program, H. Lee Moffitt Cancer Center & Research Institute, 12902 Magnolia Drive, MCC-RADONC, Tampa, FL 33612. E-mail: geoffrey.zhang@moffitt.org

**Abbreviations used in this paper:** SPECT = single photon emission computed tomography, V/Q = ventilation and perfusion.

Currently, the most common approach in thoracic radiotherapy is to generate treatment plans from computed tomography (CT) images. Other complementary imaging modalities are frequently employed as well. Positron-emission tomography (PET) has shown higher sensitivity than CT scans in detecting and staging mediastinal metastases and therefore is often used together with CT to more accurately delineate lung lesions.<sup>2,3</sup> Visible tumor on the CT images (in conjunction with PET) is contoured as the gross tumor volume, which is defined to represent macroscopic disease. To include microscopic tumor extension, radiation oncologists expand the gross tumor volume by a certain margin, which can vary in different clinical situations. This expanded volume is called clinical target volume. To account for daily treatment setup errors and tumor motion, the clinical target volume is expanded by an additional margin to form the planning target volume.

Thoracic tumors frequently move with respiration. To account for this motion, many radiation oncologists perform a 4-D CT scan. To perform such a scan requires a specially designed multislice CT scanner. The scanner employs some methodology to assess the patient's respiratory cycle during the acquisition of the CT image

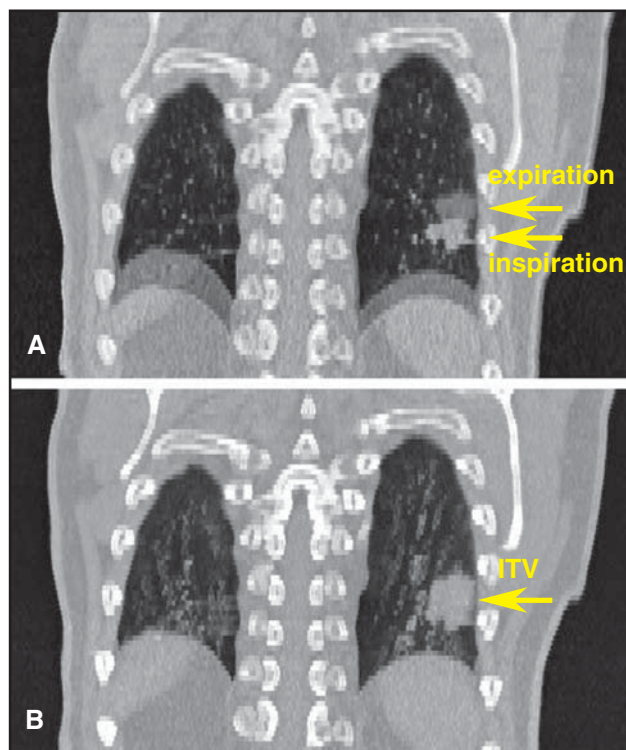


Fig 1. — The internal target volume (ITV) is determined by the maximum intensity projection (MIP) technique over the multiphase 4-D CT image set. For each voxel in the CT image frame, the maximum intensity from all phases is kept in the MIP image set. Since the intensity of a lung tumor in a CT image is higher than that of normal lung tissues, the tumor volume in the MIP image set represents the ITV. Panel A shows a superimposed view of the maximum expiration and inspiration phases. The tumor locations are indicated by the arrows. Diaphragmatic motion can also be clearly seen. Panel B shows the same view incorporating all 10 phases of the 4-D CT image set.

sets. The specific implementation varies with manufacturer, but most commonly, the patient wears an elastic belt across the upper abdomen, and the belt is attached to a pressure sensor. As the respiratory cycle progresses, tension on the sensor changes. The end result is that each CT slice is assigned to a particular point in the respiratory cycle. The included software utilizes a binning algorithm to then reconstruct a series of CT scans, equally spaced across the entire respiratory cycle. The software includes tools to generate a “CT movie” that dynamically shows tumor motion in all three planes across the respiratory cycle. When used in treatment planning, the tumor motion can be ascertained and accounted for. The volume that the clinical target volume occupies throughout the respiratory cycle is called the internal target volume (ITV). Fig 1 demonstrates a lung tumor motion assessment over a 4-D CT image set. Since the ITV already accounts for tumor motion, a margin for setup uncertainty is added to the

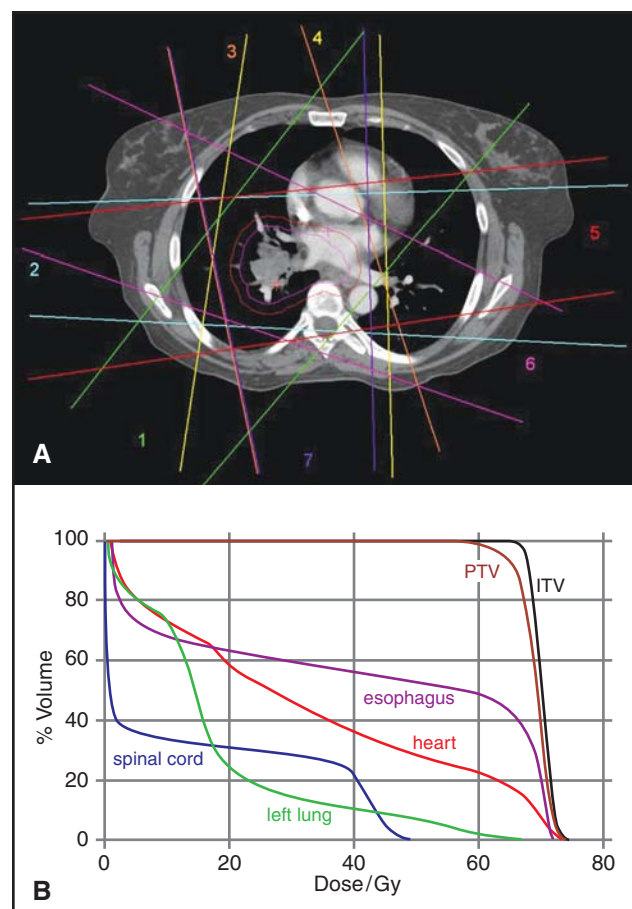


Fig 2A-B. — (A) A typical beam arrangement in an intensity-modulated radiotherapy (IMRT) plan for a lung cancer patient. In this case, 7 beams from various angles are used to cover the tumor volume. Note how the beams must pass through normal lung to reach the target. (B) The dose volume histogram (DVH) is calculated from the treatment plan. From the DVH, important parameters can be derived. For example, in this case, 95% of internal target volume (ITV) is covered by the prescribed dose of 66 Gy while 25% of the left lung receives 20 Gy. These statistics have implications in terms of tumor control as well as toxicity to normal tissues. PTV = planning target volume.

ITV to form the planning target volume. The primary goal in the treatment plan is to cover the planning target volume with a specified dose of radiation.

Studies evaluating the risks of pulmonary toxicity reported that the two best predictors were the volume of lung receiving 20 Gy or more<sup>4,5</sup> and alternatively the mean radiation dose to normal lung tissues.<sup>6</sup> Radiation traverses normal tissues to reach the tumor. This creates a necessary compromise made in treatment planning between killing tumor cells while simultaneously limiting the dose to healthy tissues to minimize pulmonary toxicity. Chronic obstructive pulmonary disease (COPD) is common in lung cancer patients. Because they typically have diminished pulmonary reserve, radiation sequelae such as pneumonitis or fibrosis can be highly morbid or even fatal.

Analogously to the lung, radiation dose constraints are placed on other critical structures such as the spinal cord, heart, and esophagus. Fig 2A demonstrates a typical radiation beam arrangement for a lung cancer intensity-modulated radiotherapy (IMRT) plan, and Fig 2B shows the dose volume histogram (DVH) for the treatment plan. The DVH is one of the tools radiation oncologists use to evaluate the treatment plan. It conveys not only the range of dose delivered to a given structure but also the volume of the structure that receives any given dose. This information can be used to estimate the toxicity of the radiation treatment plan.

When generating a DVH during the treatment planning process, the normal lung is assumed to be uniform in terms of function and particularly in terms of the ability to exchange carbon dioxide with oxygen. Anatomic variability in ventilation ( $\dot{V}$ ), defined as fractional volume change in respiration, and perfusion ( $\dot{Q}$ ), a measure of regional blood flow, are not currently considered. However,  $\dot{V}/\dot{Q}$  have substantial spatial heterogeneity. They also vary if body positioning is different<sup>7</sup> and if pulmonary diseases or malignancies are involved.<sup>8</sup> Fig 3 shows a ventilation image in supine position. Ventilation dysfunction can be seen peripheral to the tumor (purple/black regions).

Research is ongoing to incorporate  $\dot{V}/\dot{Q}$  imaging into the radiotherapy treatment planning process. At present, it is not used clinically for this purpose. However, investigations are ongoing, with the following goals: (1) to optimize radiation beam geometry to preferentially pass through dysfunctional regions of lung and maximally spare regions of normal lung function and (2) to meaningfully quantify the radiation toxicity risks by separating normal and dysfunctional regions of the lung in the dose volume histogram.

This paper reviews some commonly used clinical pulmonary functional imaging techniques. Because CT is the standard imaging modality for radiotherapy treatment planning, ongoing research into  $\dot{V}/\dot{Q}$  functional imaging using CT is most attractive to radiation oncologists;

it would obviate the need to obtain additional imaging studies. Lung motion assessment is also a goal of lung functional imaging. In radiotherapy treatment planning, however, this assessment is commonly done by generating the ITV from the 4-D CT images. Thus, our review of functional imaging is focused on  $\dot{V}/\dot{Q}$ . Motion assessment using other imaging modalities is not described.

## Ventilation and Perfusion

The major functions of the lungs are to absorb oxygen and discharge carbon dioxide. As the diaphragm depresses, the thoracic volume increases and pressure in the lungs correspondingly decreases. Air flows into lungs through the airways because of this pressure gradient. Gas exchange takes place across the extracellular matrix of a network of fine capillaries. Oxygen from the air diffuses into the bloodstream, and carbon dioxide simultaneously diffuses from the blood into the alveoli. As the diaphragm relaxes, lung volume decreases and intrathoracic pressure increases. Carbon dioxide is released from the body in the resultant expelled air.

In the gas exchange process, air flow and blood flow are the fundamental participants. Without sufficient ventilation, there is not enough oxygen for metabolic needs. Furthermore, a lack of sufficient local ventilation within the lung leads to downregulation of

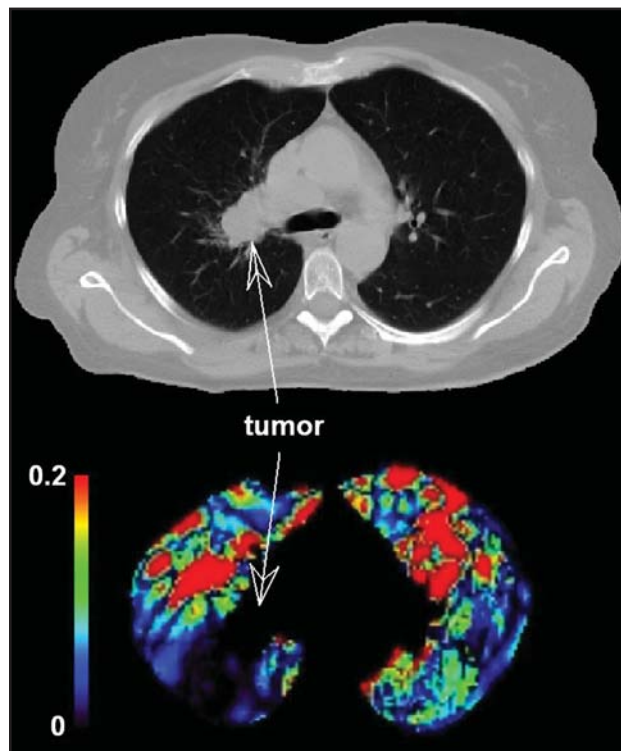


Fig 3. — Axial view of a 3-D ventilation image (lower) derived from a 4-D CT scan (upper) of a lung cancer patient. Only end expiration and inspiration phases were used in the volume change calculation. An end expiration CT image is shown. Red represents regions of high fractional volume change (high ventilation,  $dv/v \geq 0.2$ ), while black indicates no volume change ( $dv/v = 0$ ). Low ventilation regions (purple/black) can be seen peripheral to the tumor, which is expected physiologically.

perfusion in that area, triggered by hypoxic vasoconstriction. Regional ventilation can be impaired in lung cancer patients for various reasons; they frequently have underlying COPD. Advanced-stage lung tumors can also obstruct the bronchus or bronchioles, causing atelectasis distal to the obstruction. In these situations, there is a concomitant downregulation of perfusion, leading to “matched”  $\dot{V}/\dot{Q}$  defects. In contrast, reduction of perfusion (due to a pulmonary embolus, for example) does not induce regional reduction in ventilation, leading to “ $\dot{V}/\dot{Q}$  mismatch.” Radiation oncologists can exploit this difference, as noted below.

A functional assessment of lung ventilation is essentially a 2-D or 3-D map of the fractional volume change in the lungs through the respiratory cycle. A pulmonary perfusion image is a 2-D or 3-D map of blood flow. A number of different imaging modalities can be employed to analyze  $\dot{V}/\dot{Q}$ , including nuclear scintigraphy,<sup>9</sup> single photon emission computed tomography (SPECT),<sup>10-12</sup> PET,<sup>13,14</sup> magnetic resonance imaging (MRI),<sup>15</sup> and CT.<sup>16,17</sup> These are described briefly below.

## Lung Functional Imaging

### Nuclear Medicine Imaging

Nuclear medicine imaging measures the distribution and intensity of radionuclides in patients. In the course of normal body metabolic processing, specially chosen radiopharmaceuticals are preferentially absorbed by the tissue of interest and preferentially retained there. Different radiopharmaceuticals are used for different indications because of their favorable biochemical, physiologic, or metabolic properties. The most com-

mon radionuclide used in nuclear scintigraphy is <sup>99m</sup>Tc, which emits 140 keV gamma rays with a half-life of 6 hours. Other radioactive gases, such as <sup>133</sup>Xe, <sup>127</sup>Xe, <sup>81m</sup>Kr, <sup>13</sup>N, are also commonly used in pulmonary ventilation studies. Furthermore, <sup>99m</sup>Tc-diethylenetriaminepenta-acetic acid (<sup>99m</sup>Tc-DTPA) is used for lung ventilation and <sup>99m</sup>Tc-macroaggregated albumin (<sup>99m</sup>Tc-MAA) for lung perfusion imaging. PET is another nuclear medicine imaging modality. It uses specially chosen positron emitters. The most commonly used radionuclide in PET is <sup>18</sup>F.

**Scintigraphy and SPECT:** Traditionally, scintigraphy has been used for lung  $\dot{V}/\dot{Q}$  scans to assess for pulmonary embolism. A radioaerosol (<sup>99m</sup>Tc-DTPA) or radioactive gas (<sup>133</sup>Xe) is customarily employed. The scan technique determines compound utilized. For ventilation studies using the radioaerosol technique, patients breathe the <sup>99m</sup>Tc-DTPA for a few minutes while 6 to 8 static lung images are taken. The regions with low gamma ray emissions indicate low regional ventilation. When the radioactive gas technique is used, a dynamic ventilation study can be performed to assess ventilation defects over time. An initial scan is taken during or right after inhalation of the <sup>133</sup>Xe radioactive gas. Washout images are taken while the patient breathes room air. Regions of <sup>133</sup>Xe retention in the washout images indicate regional ventilation defects. Regional clearance rates can also be calculated from the scintigraphic data.

To perform a lung perfusion study, 4 to 5 mCi of <sup>99m</sup>Tc-MAA is injected. Within a few seconds after intravenous administration, over 90% of the injected dosage is trapped in the capillary and precapillary bed of the lungs. The number of particles that are trapped in a lung region is proportional to the pulmonary arterial blood flow to that region.<sup>18</sup> Conventionally, 6 to 8 images are taken. The imaging time is about 60 seconds per perfusion view. The regions of lung with low amounts of gamma radiation indicate regions of the lung with poor perfusion. Fig 4 shows an example of  $\dot{V}/\dot{Q}$  mismatch scintigraphy.

In contrast to the planar images from nuclear scintigraphy, SPECT generates 3-D images. The SPECT unit is a rotating gamma camera. Some modern SPECT models have two or even three gamma camera heads. Projection images are acquired at evenly spaced angles around the patient or continuously while rotating. In recent years, commercial manufacturers have begun to integrate CT scanners.

Fig 5 shows a Precedence SPECT/CT scanner (Philips Medical Systems, Bothell, Washington) that integrates a two-headed SPECT scanner with a 16-slice CT scanner. The CT data provide a means to calculate the attenuation of the SPECT photons by body tissues. By employing the CT data to correct the images for this attenuation, the relative intensities seen on the images

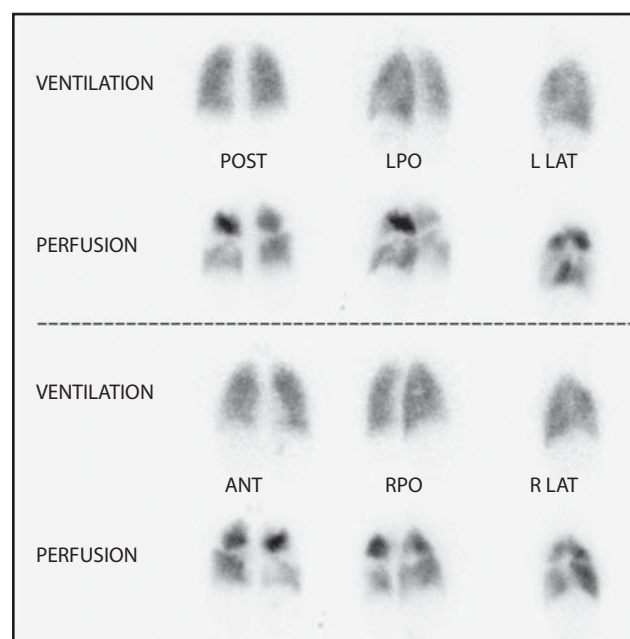


Fig 4. — Pulmonary  $\dot{V}/\dot{Q}$  mismatch as an example of  $\dot{V}/\dot{Q}$  scintigraphy. For the ventilation scan, <sup>99m</sup>Tc-DTPA was used, while <sup>99m</sup>Tc-MAA was injected for the perfusion scan. Published with permission from Barry E. Chatterton, MBBS, FRACP, DDV, of the Royal Adelaide Hospital, Australia.



Fig 5. — The Philips Precedence SPECT/CT system, which has dual-headed gamma camera and a 6- or 16-slice CT scanner. Courtesy of Philips Healthcare. <http://www.medical.philips.com>

will more accurately reflect the actual distribution of radionuclides. To further improve the spatial resolution of pulmonary SPECT scans, one can gate the ventilation scan to the respiratory cycle to acquire 4-D SPECT images. Local ventilation defects are more clearly identified when acquired at a single phase of the respiratory cycle.<sup>12</sup> Respiratory gated pulmonary perfusion images can also be obtained using SPECT.<sup>19</sup>

Dynamic pulmonary ventilation scans can also be performed with SPECT. After the radioactive gas is breath-inhaled, equilibrium and washout scans are taken in a continuous manner. Time-tagged SPECT images are reconstructed. With a dynamic SPECT study, a matrix of the half clearance time,  $T_{1/2}$ , of the radioactive gas can be calculated yielding relative ventilation maps.<sup>12</sup>

As with nuclear scintigraphy,  $^{99m}\text{Tc}$ -MAA is the main radiopharmaceutical used in perfusion studies with SPECT. SPECT perfusion scans are performed in a manner analogous to the ventilation scans, except that the radioactive contrast agent is injected and not inhaled.

**Positron-Emission Tomography:** PET is a nuclear medicine medical imaging technique that uses a short-lived positron emitter. The radioactive isotope is bound to a metabolically active molecule. The positron (an antimatter electron) annihilates when it interacts with an electron. This typically happens within 1 to 2 mm from its point of emission. This annihilation process yields a pair of 511 keV photons that are ejected in opposite directions. Special high-energy gamma detectors are distributed in rings around the patient. The detectors can identify coincident photon pairs by means of special coincidence circuits. Computerized algorithms are used to reconstruct the registered events into a 3-D image. When the PET scanner is integrated with a CT scanner, the reconstruction algorithms can utilize the CT data to account for attenuation of the photons along their paths as they traverse

bodily tissues, thereby further increasing the accuracy of the scan. There are many positron-emitting radiopharmaceuticals. The most common agent in clinical use is  $^{18}\text{F}$ -fluorodeoxyglucose (FDG), which incorporates the positron emitter into a glucose analog. The sugar is preferentially taken up by metabolically active tissues, where the positrons are emitted. While malignant tumors show preferential uptake of the compound, some benign tumors and regions of infection or inflammation can demonstrate increased FDG activity. However, because the PET scan quantifies the radiotracer concentration, malignant neoplasms can often be distinguished from nonmalignant processes. Respiratory gating is sometimes used in modern FDG-PET imaging to reduce the motion artifact in the lung and to improve detection of small malignant lesions.<sup>20,21</sup> Other commonly used positron-emitting radionuclides include  $^{11}\text{C}$ ,  $^{15}\text{O}$  and  $^{82}\text{Rb}$ .

$\dot{V}/\dot{Q}$  studies can be performed simultaneously with intravenous infusion of  $^{13}\text{N}_2$ .<sup>13,22</sup> The patient holds his or her breath for a short period of time while receiving the compound. The alveolar concentration of the tracer increases until a plateau is reached. When the subject resumes breathing, the washout phase starts and the concentration decreases as the tracer is removed by ventilation. Since  $^{13}\text{N}_2$  absorption to pulmonary venous blood during the apnea is negligible, the regional tracer content during apnea is proportional to regional perfusion. Since  $^{13}\text{N}_2$  is eliminated from the lung almost exclusively by ventilation when the subject resumes breathing, ventilation can be assessed using the washout data.

### Magnetic Resonance Imaging

MRI is a widely used imaging modality in radiotherapy treatment planning. It is particularly advantageous for imaging soft tissues such as muscle or brain. The images can be fused with those from the radiation treatment planning CT scan to assist the radiation oncologist in defining appropriate tumor volumes. For the principle and technical details of MRI, many textbooks and scientific journals are good resources.<sup>23,24</sup> MRI provides two main advantages in pulmonary functional imaging: (1) it does not rely on ionizing radiation, and (2) it provides higher spatial resolution than nuclear medicine imaging. High temporal resolution can be reached if images of a single slice or small volume are acquired.<sup>25</sup>

A common approach of MRI-based pulmonary  $\dot{V}/\dot{Q}$  assessment uses gadolinium-based contrast agents. Since the 1980s, MRI studies have investigated the use of aerosolized gadolinium chelates (Gd-DTPA) in lung ventilation imaging.<sup>26-28</sup> In lung perfusion imaging, gadopentetate dimeglumine (Magnevist, Berlex Laboratories, Wayne, New Jersey) is given as a bolus injection.<sup>25</sup> Gd-DTPA aerosol and electrocardiogram (ECG)-gated MRIs are also used in pulmonary perfusion studies.<sup>15</sup>

Oxygen enhancement is another MRI-based approach. There is a substantial difference in oxygen partial pressure when breathing room air, 20% oxygen, and pure oxygen. Because of the enormous surface area of the lattice of alveoli, the effect of molecular oxygen on MRIs is significant despite the fact that it is only weakly paramagnetic. The signal intensity increases by about 15% when subtracting room air breathing images from pure oxygen breathing images.<sup>29</sup>  $\dot{V}/\dot{Q}$  studies can be performed with this technique, though this modality cannot capture dynamic changes. Other MRI-based pulmonary  $\dot{V}/\dot{Q}$  research uses hyperpolarized noble gases.<sup>30,31</sup>

### Computed Tomography

Usually CT pulmonary functional imaging incorporates iodine-based radiocontrast agents.<sup>17,32,33</sup> The radiocontrast is bright on CT images, permitting assessment of vascular structures. As the spatial resolution of CT and the x-ray tube technology improves, a newer pulmonary perfusion assessment technique using dual-source/dual-energy CT holds increasing promise.<sup>17</sup> In a Somatom Definition dual-source CT scanner (Siemens Medical Systems, Forchheim, Germany), two x-ray tubes are offset from one another by 90° (Fig 6). Two CT image sets of different x-ray energies are acquired simultaneously. The grey levels in CT images depend on the magnitude of the x-ray attenuation that is determined both by the composition of the tissue (its electron density) and the x-ray energy. The differences in attenuation between the two CT image sets of different x-ray energies give a much better differentiation of tissue composition. The iodine radio-

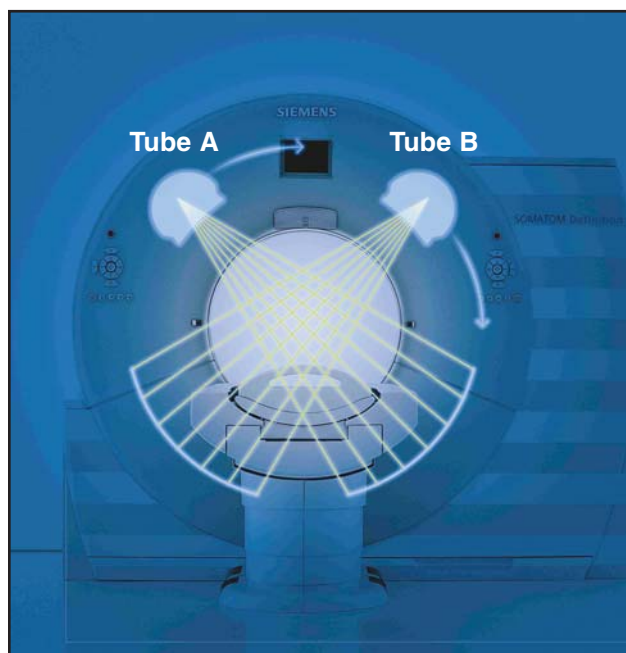


Fig 6. — Two x-ray tubes of different energies are offset by 90° in a dual-source CT scanner. Courtesy of Siemens Zrt. <http://www.siemens.hu/>

contrast material, which is of high atomic number, is thus clearly differentiated from other tissues in the dual-source CT images. Johnson et al<sup>17</sup> used 80 and 140 kilovolt peak (kVp) for the dual sources, and the current of the 80 kVp tube was 3 times that of the 140 kVp tube to compensate for the low x-ray output due to low tube voltage.

Guerrero et al<sup>16</sup> suggested a pulmonary ventilation imaging algorithm using a 4-D CT and deformable image registration. A 4-D CT scan is a series of complete CT image sets, each taken at a particular point in the respiratory cycle. Deformable image registration provides a voxel-to-voxel deformation matrix among CT images from different phases of the respiratory cycle. The deformable image registration can be used to quantify the density change within a particular voxel over the time course of the respiratory cycle. The corresponding density changes (Hounsfield unit changes) represent a quantification of pulmonary ventilation. It is well known that ventilation of the lungs is not uniform.<sup>7,34</sup> By generating a colorwash from the matrix of CT number differences, a 2-D image of lung ventilation is generated (Fig 3).

Four-dimensional CT-based lung functional imaging is not employed clinically. Whole-lung dynamic  $\dot{V}/\dot{Q}$  imaging using the radiocontrast technique is not routinely utilized due to the long image acquisition time. Ongoing research into ventilation studies using 4-D CT images may lead to a breakthrough in CT-based lung functional imaging. The technique is attractive because 4-D CT is already commercially available from at least two vendors. Therefore, since 4-D CT is increasingly employed by radiation oncologists, no additional imaging studies are required to assess pulmonary function, thus reducing both cost and time for the patient. The dynamic ventilation information is inherent within the multiphase images with temporal resolution of less than a half second. High spatial resolution can be achieved, which is a major advantage over SPECT.

Research is ongoing to overcome some technical challenges. For example, the 4-D CT imaging artifact, ie, the residual motion in each respiratory phase, is the major source of errors in the deformable image registration. Any mismatched registration, especially around regions of high density such as blood vessels in the lungs can cause errors in the resultant ventilation image. More robust computational algorithms are necessary to reduce such errors. These are currently under investigation.

### Imaging for Thoracic Radiation Oncology

CT is the standard imaging modality in radiotherapy treatment planning. It provides both detailed anatomical visualization and the means to perform accurate radiation dose distribution calculations. The physics principles underlying CT scans involve the concept of

electron density, which likewise determines the distribution of therapeutic radiation dose in tissue. The details are beyond the scope of this article but are available elsewhere.<sup>23,35,36</sup> Within the treatment planning software, using the CT images, radiation oncologists can place shaped radiation beams onto tumors and accurately determine the resultant dose distribution within the patient. During the treatment planning process, the dosimetrist contours normal anatomic structures of interest (lung, esophagus, heart, spinal cord). When treatment beams are placed onto the patient in the treatment planning software, the dose to normal tissues can be calculated and a dose volume histogram can be generated.

Researchers have proposed using pulmonary  $\dot{V}/\dot{Q}$  images in radiotherapy treatment planning.<sup>37,38</sup> Clinically, the  $\dot{V}/\dot{Q}$  images are currently performed using SPECT. The functional SPECT images are then fused with the treatment planning CT images. The normal functional lung volumes are then contoured onto the planning CT images. Radiation dose objectives are placed on the normal lung volumes during the treatment planning process. The resultant plan not only provides appropriate radiation dose coverage to the tumor but also maximally spares normal functional lung.

Most cancer patients receiving radiotherapy undergo CT imaging for treatment planning. To include functional lung sparing, patients require SPECT or dual-source/dual-energy CT images in addition to the radiation treatment planning CT scan, adding both extra cost and inconvenience. Since almost all lung cancer patients have matched  $\dot{V}/\dot{Q}$  defects, either functional ventilation or perfusion imaging alone should be sufficient to assess lung function. Since many radiation oncologists routinely use 4-D CT scans to assess tumor motion throughout the respiratory cycle, ongoing research into ventilation imaging using 4-D CT image sets has garnered the most attention from radiation oncologists. It is hoped that this will soon be commonplace to quantify regional variability in lung ventilation with deformable image registration. If it were possible to differentiate regions of functional lung, radiation oncologists could preferentially spare the functioning lung.<sup>39</sup> It might then be possible to safely escalate radiation dose in patients and improve disease control.

## Conclusions

Like the case of tumor motion assessment, pulmonary  $\dot{V}/\dot{Q}$  imaging shows promise in generating better radiotherapy treatment plans for lung cancer patients, sparing functional lung while simultaneously delivering sufficient radiation dose to the tumors. Many pulmonary functional imaging techniques have potential application in radiation oncology. The use of 4-D CT is most promising, for both its convenience and its advantage in spatial resolution.

## Disclosures

*No significant relationship exists between the authors and the companies/organizations whose products or services may be referenced in this article.*

*The editor of Cancer Control, John Horton, MB, CbB, FACP, has nothing to disclose.*

## References

1. American Cancer Society. *Cancer Facts & Figures, 2007*. Atlanta, GA: American Cancer Society; 2007.
2. Chin R Jr, Ward R, Keyes JW, et al. Mediastinal staging of non-small-cell lung cancer with positron emission tomography. *Am J Respir Crit Care Med*. 1995;152(6 pt 1):2090-2096.
3. Erdi YE, Rosenzweig K, Erdi AK, et al. Radiotherapy treatment planning for patients with non-small cell lung cancer using positron emission tomography (PET). *Radiother Oncol*. 2002;62:51-60.
4. Graham MV, Purdy JA, Emami B, et al. Clinical dose-volume histogram analysis for pneumonitis after 3D treatment for non-small cell lung cancer (NSCLC). *Int J Radiat Oncol Biol Phys*. 1999;45:323-329.
5. Lee HK, Vaporciyan AA, Cox JD, et al. Postoperative pulmonary complications after preoperative chemoradiation for esophageal carcinoma: correlation with pulmonary dose-volume histogram parameters. *Int J Radiat Oncol Biol Phys*. 2003;57:1317-1322.
6. Marks LB, Munley MT, Spencer DP, et al. Quantification of radiation-induced regional lung injury with perfusion imaging. *Int J Radiat Oncol Biol Phys*. 1997;38:399-409.
7. Glenn RW, Bernard S, Robertson HT, et al. Gravity is an important but secondary determinant of regional pulmonary blood flow in upright primates. *J Appl Physiol*. 1999;86:623-632.
8. Nakagawa T, Sakuma H, Murashima S, et al. Pulmonary ventilation-perfusion MR imaging in clinical patients. *J Magn Reson Imaging*. 2001;14:419-424.
9. Gottschalk A, Sostman HD, Coleman RE, et al. Ventilation-perfusion scintigraphy in the PLOPED study. Part II. Evaluation of the scintigraphic criteria and interpretations. *J Nucl Med*. 1993;34:1119-1126.
10. Harris B, Bailey D, Miles S, et al. Objective analysis of tomographic ventilation-perfusion scintigraphy in pulmonary embolism. *Am J Respir Crit Care Med*. 2007;175:1173-1180. Epub 2007 Mar 15.
11. Petersson J, Sánchez-Crespo A, Rohdin M, et al. Physiological evaluation of a new quantitative SPECT method measuring regional ventilation and perfusion. *J Appl Physiol*. 2004;96:1127-1136. Epub 2003 Nov 14.
12. Suga K. Technical and analytical advances in pulmonary ventilation SPECT with xenon-133 gas and Tc-99m-Technegas. *Ann Nucl Med*. 2002;16:303-310.
13. Vidal Melo MF, Layfield D, Harris RS, et al. Quantification of regional ventilation-perfusion ratios with PET. *J Nucl Med*. 2003;44:1982-1991.
14. Musch G, Layfield JD, Harris RS, et al. Topographical distribution of pulmonary perfusion and ventilation, assessed by PET in supine and prone humans. *J Appl Physiol*. 2002;93:1841-1851.
15. Ogasawara N, Suga K, Kawakami Y, et al. Assessment of regional lung function impairment in airway obstruction and pulmonary embolic dogs with combined noncontrast electrocardiogram-gated perfusion and gadolinium diethylenetriaminepentaacetic acid aerosol magnetic resonance images. *J Magn Reson Imaging*. 2004;20:46-55.
16. Guerrero T, Sanders K, Castillo E, et al. Dynamic ventilation imaging from four-dimensional computed tomography. *Phys Med Biol*. 2006;51:777-791. Epub 2006 Jan 25.
17. Johnson TR, Krauss B, Sedlmair M, et al. Material differentiation by dual energy CT: initial experience. *Eur Radiol*. 2007;17:1510-1517. Epub 2006 Dec 7.
18. Wagner HN. Regional ventilation and perfusion. In: Wagner HN Jr, Szabo Z, Buchanan JW, eds. *Principles of Nuclear Medicine*. 2nd ed. Philadelphia, PA: WB Saunders; 1995:881-895.
19. Suga K, Kawakami Y, Zaki M, et al. Pulmonary perfusion assessment with respiratory gated 99mTc macroaggregated albumin SPECT: preliminary results. *Nucl Med Commun*. 2004;25:183-193.
20. Boucher L, Rodrigue S, Lecomte R, et al. Respiratory gating for 3-dimensional PET of the thorax: feasibility and initial results. *J Nucl Med*. 2004;45:214-219.
21. Nehmeh SA, Erdi YE, Ling CC, et al. Effect of respiratory gating on quantifying PET images of lung cancer. *J Nucl Med*. 2002;43:876-881.
22. Schuster DP, Anderson C, Kozlowski J, et al. Regional pulmonary perfusion in patients with acute pulmonary edema. *J Nucl Med*. 2002;43:863-870.
23. Bushberg JT, Seibert JA, Leidholdt EM Jr, et al, eds. *The Essential Physics of Medical Imaging*. 2nd ed. Philadelphia, PA: Lippincott Williams & Wilkins; 2002.
24. Peters TM, Slomka PJ, Fenster A. Imaging for radiation therapy planning (MRI, nuclear medicine, ultrasound). In: van Dyke J, ed. *The Modern*

*Technology of Radiation Oncology*. Vol 1. Madison, WI: Medical Physicist Publishing; 1999:191-229.

25. Levin DL, Chen Q, Zhang M, et al. Evaluation of regional pulmonary perfusion using ultrafast magnetic resonance imaging. *Magn Reson Med*. 2001;46:166-171.

26. Misselwitz B, Mühler A, Heinzlmann I, et al. Magnetic resonance imaging of pulmonary ventilation. Initial experiences with a gadolinium-DTPA-based aerosol. *Invest Radiol*. 1997;32:797-801.

27. Montgomery AB, Paajanen H, Brasch RC, et al. Aerosolized gadolinium-DTPA enhances the magnetic resonance signal of extravascular lung water. *Invest Radiol*. 1987;22:377-381.

28. Suga K, Yuan Y, Ogasawara N, et al. Altered clearance of gadolinium diethylenetriaminepentaacetic acid aerosol from bleomycin-injured dog lungs. *Am J Respir Crit Care Med*. 2003;167:1704-1710. Epub 2003 Feb 20.

29. Löffler R, Müller C, Peller M, et al. Optimization and evaluation of the signal intensity change in multisection oxygen-enhanced MR lung imaging. *Magn Reson Med*. 2000;43:860-866.

30. Kauczor H, Surkau R, Roberts T. MRI using hyperpolarized noble gases. *Eur Radiol*. 1998;8:820-827.

31. Möller HE, Chen XJ, Saam B, et al. MRI of the lungs using hyperpolarized noble gases. *Magn Reson Med*. 2002;47:1029-1051.

32. Flohr TG, McCollough CH, Bruder H, et al. First performance evaluation of a dual-source CT (DSCT) system. *Eur Radiol*. 2006;16:256-268. Epub 2005 Dec 10.

33. Sreaton NJ, Coxson HO, Kaloger SE, et al. Detection of lung perfusion abnormalities using computed tomography in a porcine model of pulmonary embolism. *J Thorac Imaging*. 2003;18:14-20.

34. Altemeier WA, McKinney S, Glenn RW. Fractal nature of regional ventilation distribution. *J Appl Physiol*. 2000;88:1551-1557.

35. Herman GT, ed. *Image Reconstruction From Projections: The Fundamentals of Computerized Tomography*. New York, NY: Academic Press; 1980.

36. van Dyke J, Taylor JS. CT simulators. In: van Dyke J, ed. *The Modern Technology of Radiation Oncology*. Vol 1. Madison, WI: Medical Physics Publishing; 1999:131-168.

37. Lavrenkov K, Christian JA, Partridge M, et al. A potential to reduce pulmonary toxicity: the use of perfusion SPECT with IMRT for functional lung avoidance in radiotherapy of non-small cell lung cancer. *Radiother Oncol*. 2007;83:156-162. Epub 2007 May 9.

38. Shioyama Y, Jang SY, Liu HH, et al. Preserving functional lung using perfusion imaging and intensity-modulated radiation therapy for advanced-stage non-small cell lung cancer. *Int J Radiat Oncol Biol Phys*. 2007;68:1349-1358. Epub 2007 Apr 18.

39. Yaremko BP, Guerrero TM, Noyola-Martinez J, et al. Reduction of normal lung irradiation in locally advanced non-small-cell lung cancer patients, using ventilation images for functional avoidance. *Int J Radiat Oncol Biol Phys*. 2007;68:562-571. Epub 2007 Mar 29.